Implantation Doping of GaN

J. C. Zolper

Sandia National Laboratories, Albuquerque, NM 87185-0603

Ion implantation has played an enabling role in the realization of many high performance photonic and electronic devices in mature semiconductor materials systems such as Si and GaAs. This can also be expected to be the case in III-Nitride based devices as the material quality continues to improve. This paper reviews the progress in ion implantation processing of the III-Nitride materials, namely, GaN, AlN, InN and their alloys. Details are presented of the successful demonstrations of implant isolation as well as n- and p-type implantation doping of GaN. Implant doping has required activation annealing at temperatures in excess of 1000 °C. The nature of the implantation induced damage and its response to annealing is addressed using Rutherford Backscattering. Finally, results are given for the first demonstration of a GaN device fabricated using ion implantation doping, a GaN junction field effect transistor (JFET).

INTRODUCTION

The III-Nitride material system has been the focus of extensive research for application to ultraviolet emitters and detectors (1,2). In addition, this material system is attractive for use in high-temperature or high-power electronic devices (3,4). A primary reason for the recent advances in III-N based photonic devices was the demonstration of p-type doping of GaN during metal organic chemical vapor deposition (MOCVD) growth followed by a dehydrogenation anneal to activate the Mg acceptors (5,6). Moreover, since ion implantation has been the foundation of most advanced electronic and, to a lesser extent, photonic devices in mature semiconductor materials systems such as silicon and gallium arsenide(7) it is important to determine the applicability of ion implantation to III-Nitride based devices. In particular the demonstration of selective area implant isolation and doping will allow new III-Nitride based device structures such as lasers and FETs with selectively doped contact regions, planar waveguides created by implant isolation, and implantation tailored current guiding in light emitting diodes (LEDs) and lasers, to name a few. In this paper, we present results for the successful n- and p-type implant doping of GaN that lead to the first GaN junction field effect transistor (JFET). The JFET was produced with all ion implantation doping. Details for the implantation induced damage in GaN and its response to high temperature annealing is also presented.

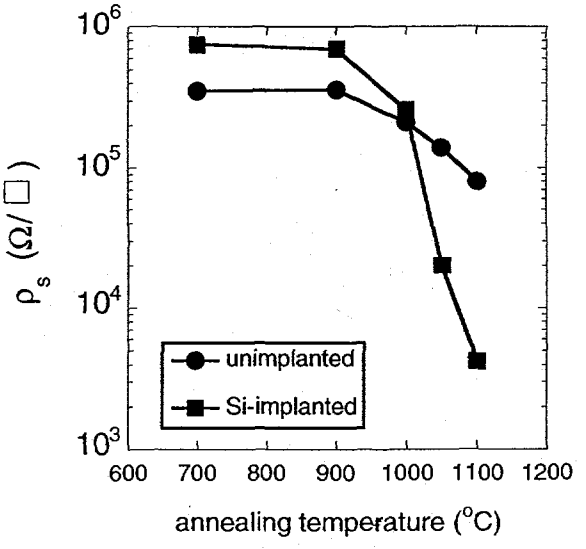

Fig 1. Sheet resistance versus annealing temperature for Si-implanted (200 keV, $5e10^{14}$ cm^{-2}) and unimplanted GaN. Activation of the Si-donors begins after a 1050 °C anneal with increased activity after 1100 °C.

N- AND P-TYPE IMPLANT DOPING

Figure 1 shows the evolution of sheet resistance versus annealing temperature for Si-implanted (200 keV, $5x10^{14}$ cm^{-2}) and unimplanted GaN (8). The samples were annealed for 10 s in flowing N_2 in a silicon carbide coated graphite susceptor. It is critical to use a hydrogen free ambient to avoid hydrogen passivation of the dopants and thus to achieve electrical activity. The presence of hydrogen during the anneal will also cause decomposition of the GaN surface though the formation of NH_3 (9). As seen in Fig. 1, electrical activity starts to occur at 1050 °C,

DISCLAIMER

as evident by the drop in sheet resistance, and further increases at 1100 °C.

Figure 2 shows the evolution of sheet resistance versus annealing temperature (10 s rapid thermal anneals) for Mg (180 keV, $5x10^{14}$ cm^{-2}), Mg+P (180/250 keV, both $5x10^{14}$ cm^{-2}), and unimplanted GaN. The Mg-only samples remain n-type up to 1100 °C while the Mg samples co-implanted with ^{31}P convert from n-to-p type after a 1050 °C anneal. The effect of the ^{31}P co-implantation may be explained by a reduction of nitrogen-vacancies or an increase in Ga-vacancies leading to a higher probability of Mg occupying a Ga-site. Co-implantation of P has also been shown to be effective in enhancing activation and reducing diffusion for p-type implantation in GaAs (10). The ionization levels of implanted Mg has also been determined from an Arrhenius plot of carrier density to be 171 meV and is consistent with the value reported for epitaxial Mg-doped GaN (11,1).

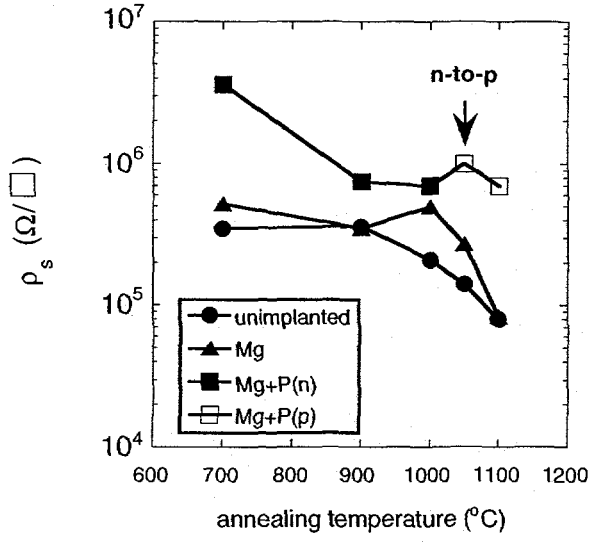

FIGURE 2. Sheet resistance versus annealing temperature for Mg-implanted (180 keV, $5e10^{14}$ cm^{-2}), Mg+P (180/250 keV, $5e10^{14}$ cm^{-2}) implanted, and unimplanted GaN. The Mg+P samples convert from n-to-p type after a 1050 °C anneal with an increased hole density after annealing at 1100 °C. The Mg-only samples remain n-type for all annealing temperatures.

Since the ionization level of Mg in GaN is much greater than the thermal energy, kT, less than 1% of the Mg-acceptors will be ionized at room temperature. Therefore, it would be desirable to identify an acceptor species with a smaller ionization energy. Since Ca has been suggested theoretically to be a shallow acceptor in GaN (12); ion implantation was used to determine the ionization energy of Ca in GaN (13). Figure 3 shows the evolution of sheet resistance versus annealing temperature (10 s rapid thermal anneals) of Ca (180 keV, $5x10^{14}$ cm^{-2}), Ca+P (180/130 keV, both $5x10^{14}$ cm^{-2}), and unimplanted GaN. Both the Ca-only and the Ca+P samples converted from n-to-p type after a 1100 °C anneal with a further increase in p-type conduction after a 1150 °C anneal. The fact that P co-implantation is not required to achieve p-type conductivity with Ca can be understood based on the higher mass of the Ca-ion, as compared to Mg, generating more implantation damage and therefore more Ga-vacancies. This explanation is supported by the higher activation temperature required for conversion from n-to-p type for the Ca-implanted samples compared to the Mg+P implanted samples. The ionization level of Ca was estimated from an Arrhenius plot to be 169 meV (13), which is equivalent to that of Mg. Although the ionization level of Ca is not less than that of Mg, Ca may be preferred for forming shallow implanted p-regions in GaN due to its heavier mass and resulting smaller projected range and straggle than Mg for a given energy.

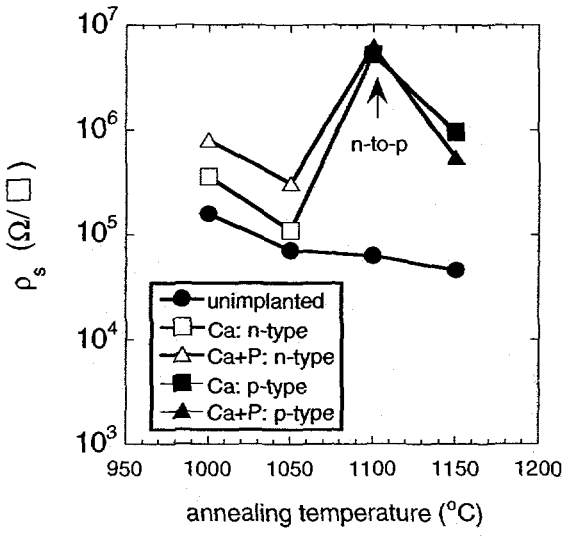

FIGURE 3. Sheet resistance versus annealing temperature for Ca-implanted (180 keV, $5e10^{14}$ cm^{-2}), Ca+P (180/130 keV, $5e10^{14}$ cm^{-2}) implanted, and unimplanted GaN. Both the Ca-only and the Ca+P samples convert from n-to-p type after a 1100 °C anneal with an increased hole density after annealing at 1150 °C.

IMPLANT ISOLATION

Ion implantation can also be used to convert initially conducting regions to high resistance regions for device isolation or current guiding. Figure 4 shows sheet resistance versus annealing temperature for initially n- and p-type GaN implanted with N. N-implantation is seen to effectively compensates both p- and n-type material (8). For both doping types the resistance first increases with annealing temperature then reaches a maximum before demonstrating a significant reduction in resistance after a

850 °C anneal for n-type and a 950 °C anneal for p-type GaN. This behavior is typical of implant-damage compensation. The energetic positions of the defect levels from the respective bands are estimated from Arrhenius plots of the resistance/temperature product to be 0.83 eV for initially n-type and 0.90 eV for initially p-type GaN (8). These levels are still not at midgap, but are sufficiently deep to realize a sheet resistance > 10^9 Ω/□. He implantation has also been reported to effectively isolate n-type GaN, with the material remaining compensated to over 850 °C (14). Interestingly, H-implant compensation of n-type GaN is reported to anneal out at ~400 °C with an anomalous dependenceon implant energy (14).

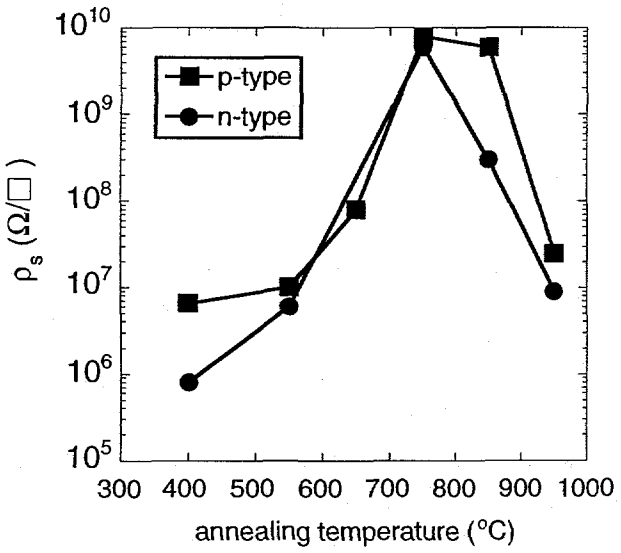

FIGURE 4. Sheet resistance versus annealing temperature for N-implanted initially n- and p-type GaN. The N was implanted at multiple energies to give an approximately uniform ion concentration of $4x10^{18}$ cm^{-3} across ~500 nm.

IMPLANTATION DAMAGE

To further study the implant induced damage, channeling Rutherford Backscattering (C-RBS) and cross-sectional transmission electron spectroscopy (XTEM) were performed on selected samples (15-17). Figure 5a shows the C-RBS spectra for Si-implanted GaN versus implant dose. The implantation-induced damage is barely visible in the channeling spectra until a dose of $2.2x10^{15}$ cm^2 is reached. In addition, an amorphous region does not form until a dose of $2.4x10^{16}$ cm^{-2} is reached. This dose threshold for measurable damage formation and amorphization is significantly higher than for other III-V semiconductors.

Figure 5b shows the change in the RBS spectra between the as-implanted sample for a dose of $6x10^{15}$ cm^{-2} and the same sample annealed at 1100 C for 30 s. When changes in the near surface scattering and dechanneling are accounted for, there is little reduction in the subsurface damage (15). This has been confirmed by XTEM images of as-implanted (Si: $6x10^{15}$ cm^{-2}) and annealed (1100 °C, 30 s) GaN.

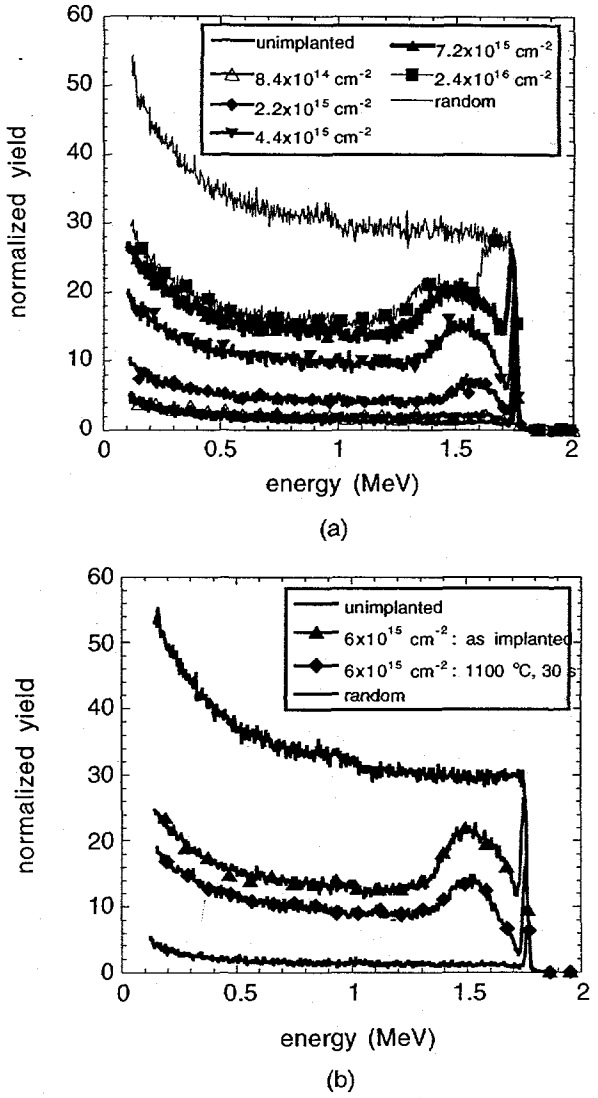

FIGURE 5. Channeling Rutherford Backscattering spectra for a) Si-implanted GaN versus dose and b) as-implanted ($6x10^{15}$ cm^{-2}) and annealed (1100 °C, 30 s) GaN.

GaN JFET

As discussed earlier, ion implantation doping and isolation has played a critical role in the realization of many high performance devices in most mature semiconductor materials systems such as Si and GaAs. This is also expected to be the case for III-Nitride based

devices as the quality of the III-N materials continues to improve. Even though the III-Nitride materials are far from mature, all ion implanted transistors have already been demonstrated (18).

Figure 6 shows the I_{DS} versus V_{DS} curves for varied gate biases for a ~1.7 μm x 50 μm GaN JFET with a 4 μm source-to-drain spacing fabricated with a Si-implanted n-type channel and source/drain regions and Ca-implanted p-type gate. The JFET demonstrates good modulation characteristics with nearly complete pinch-off at a threshold voltage of approximately -6 V for V_{DS} = ~7V. For V_{DS} = 25 V, a maximum transconductance of 7 mS/mm was measured at V_{GS} = -2.0 V with a saturation current of 33 mA/mm at V_{GS} = 0 V. These devices had a unity current gain cutoff frequency (f_t) of 2.7 GHz and a maximum oscillation frequency (f_{max}) of 9.4 GHz at V_{GS} = 0 V and V_{DS} = 25 V. These frequency metrics are in the range reported for epitaxial GaN MESFETs (19).

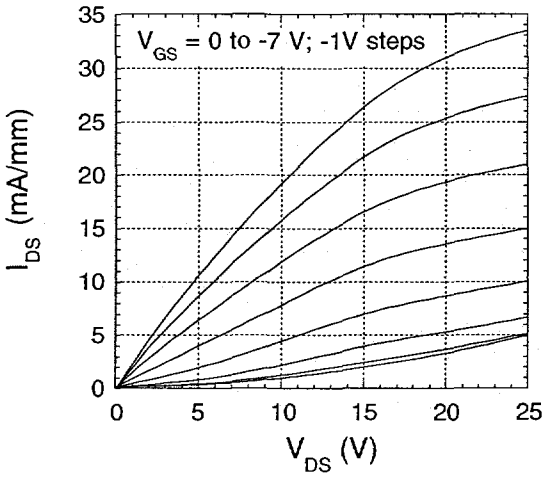

FIGURE 6. I_{DS} versus V_{DS} for varied V_{GS} for a 0.7x50 μm² all ion implanted GaN JFET.

CONCLUSION

As with other semiconductor material systems, ion implantation is expected to play an enabling role for advanced device fabrication in the III-Nitride material system. As reported here, ion implantation has already been used to achieve n- and p-type doping of GaN and to fabricate the first GaN JFET. As further understanding is obtained on implantation induced defects, activation annealing, and the role of other impurities in these materials, it is anticipated that ion implantation will be more widely used for III-Nitride devices.

ACKNOWLEDGMENT

The work performed at Sandia was supported by the DOE under contract #DE-ACO4-94AL85000. The assistance of S. J. Pearton of the Un. of Florida and J. S. Williams of the Australian National University is gratefully appreciated. The contribution of GaN material from Emcore Corporation (R. A. Stall) is also acknowledged.

REFERENCES

1. I. Akasaki, H. Amano, M. Kito, and K. Hiramatsu, J. Lumin. **48/49** 666 (1991).
2. S. Nakamura, T. Mukai, and M. Senoh, Appl. Phys. Lett. **64**, 1687 (1994).
3. M. A. Khan, A. Bhattarai, J. N. Kuznia, and D. T. Olson, Appl. Phys. Lett. **63**, 1214 (1993).
4. S. C. Binari, L. B. Rowland, W. Kruppa, G. Kelner, K. Doverspike, and D. K. Gaskill, Elect. Lett. **30**, 1248 (1994).
5. H. Amano, M. Kito, K. Hiramatsu, and I. Akasaki, Jap. J. Appl. Phys. **28** L2112 (1989).
6. S. Nakamura, T. Mukai, M. Senoh, and N. Iwasa, Jap. J. Appl. Phys. **31** L139 (1992).
7. see for example: J. F. Ziegler, ed., Handbook of Ion Implantation Technology (Elsevier Science Publishers, The Netherlands, 1992) pp. 271-362; S. K. Ghandi, VSLI Fabrication Principles: Silicon and Gallium Arsenide (John Wiley & Sons, New York, 1982) chapter 6.
8. S. J. Pearton, C. R. Abernathy, C. B. Vartuli, J. C. Zolper, C. Yuan, R. A. Stall, Appl. Phys. Lett. **67**, 1435 (1995).
9. C. J. Sun, P. Kung, A. Saxler, H. Ohsato, E. Bigan, M. Razeghi, and D. K. Gaskill, J. Appl. Phys. **76**, 236 (1994).
10. M. E. Sherwin, J. C. Zolper, A. G. Baca, T. J. Drummond, R. J. Shul, A. J. Howard, D. J. Rieger, R. P Schneider, and J. F. Klem, J. Elec. Mater. **15**, 809 (1994).
11. J. C. Zolper, M. Hagerott Crawford, S. J. Pearton, C. R. Abernathy, C. B. Vartuli, C. Yuan, and R. A. Stall, J. Electron. Mat. **25**, 839 (1996).
12. S. Strite, Jpn. J. Appl. Phys. **33**, L699 (1994).
13. J. C. Zolper, R. G. Wilson, S. J. Pearton, and R. A. Stall, Appl. Phys. Lett. **68**, 1945 (1996).
14. S. C. Binari, H. B. Dietrich, G. Kelner, L. B. Rowland, K. Doverspike, D. K. Wickenden, J. Appl. Phys. **78**, 3008 (1995).
15. H. H. Tan, J. S. Williams, J. Zou, D. J. H. Cockayne, S. J. Pearton, and R. A. Stall, Appl Phys Lett. (in press).
16. H. H. Tan, J. S. Williams, J. Zhou, D. J. H. Cockayne, S. J. Pearton, and C. Yuan, Conf. Proceedings Spring 1996 Electrochemical Society Meeting, Los Angles, CA, May 5-10, 1996 (in press).
17. J. C. Zolper, M. H. Crawford, J. S. Williams, H. H. Tan, and R. A. Stall, Conf. Record Ion Beam Modification of Materials, Sept. 1-6, 1996, Albuquerque, NM.
18. J. C. Zolper, R. J. Shul, A. G. Baca, R. G. Wilson, S. J. Pearton, and R. A. Stall, Appl. Phys. Lett. **68**, 2273 (1996).
19. S. C. Binari, Proc. Sym. on Wide Bandgap Semiconductors and Devices, Fall ECS meeting 1995 (The Electrochemical Society, Pennington, NJ, 1995) p. 136.